Proceedings of the 9th U.S. National and 10th Canadian Conference on Earthquake Engineering
Compte Rendu de la 9ième Conférence Nationale Américaine et
10ième Conférence Canadienne de Génie Parasismique
July 25-29, 2010, Toronto, Ontario, Canada • Paper No 1018

CODES OF ASSESSMENT OF BUILDINGS: A COMPARATIVE STUDY

S. G. Chassioti[1], D. V. Syntzirma[2] and S. J. Pantazopoulou[3]

ABSTRACT

In displacement based design, the so-called *acceptance criteria* ride on the ability to assess with confidence the deformation capacity of the individual members of a structure. Codes of assessment of existing structures (Eurocode 8-(Part III) and FEMA 356 and 440) provide a relatively complex procedure for evaluation of deformation capacity; however, contrary to strength estimations, deformation capacity estimates demonstrate a significant degree of dispersion with respect either experimental databases or analytical models, particularly when used to evaluate lightly reinforced members representative of older construction practices in North America and Europe up to the 80's. In this paper a benchmark test is introduced and proposed to be used for evaluation and comparison of deformation components estimated with either mechanical models or Code expressions. The paper summarizes the first principles underlying the mechanical problem of deformation capacity calculation, the basic Code Models established in the US and European assessment practice, and comparatively evaluates the performance of these three alternatives with reference to the proposed Benchmark test, in order to illustrate the parameters responsible for the scatter and uncertainty in the evaluated results.

Introduction

This paper critically reviews the available methods of assessment of deformation capacity of reinforced concrete (R.C.) prismatic members, with particular emphasis on Code expressions recommended for use in displacement-based assessment of existing structures. Of particular concern are lightly reinforced prismatic concrete members typically found in substandard construction built prior to the introduction of modern seismic detailing. Such members are susceptible to premature modes of failure prior to the realization of the full deformation capacity which would be normally estimated based on classical mechanics of flexural response.

As the deformation capacity estimates obtained using the Codes of Assessment against test data generally illustrate a poor predictive capacity, a comparative study is conducted in this paper considering the estimated deformation capacities obtained from a model developed from first principles (Syntzirma and Pantazopoulou 2006), with the estimates obtained from

[1] Civil Engineer, Dept. of Civil Engineering, Demokritus Univ. Thrace, Greece, stamchas@civil.duth.gr
[2] PhD, M.Sc., Civil Engineer, Dept. of Civil Engineering, Demokritus Univ.of Thrace, Greece, dsyntz@civil.duth.gr
[3] Professor, Dept. of Civil Engineering, Demokritus Univ. of Thrace, Vas. Sofias 12A, Xanthi 67100, Greece, +30−25410−79639, pantaz@civil.duth.gr

recommended seismic code procedures. A series of column-elements are examined; these represent various practical problems of old construction with substandard details, typically encountered in assessment practice and termed ***non-conforming*** as per FEMA 356 (2000). The collection of example cases considered, are proposed in this paper as a benchmark test for comparative evaluation of alternative methods and definitions of deformation capacity for seismic assessment and design.

Definition and modelling of deformation mechanisms in R.C. members

The behaviour of R.C. frame members under combined axial load, cyclic shear and flexure, such as occurring during earthquakes, is usually interpreted with the cantilever model depicted in Fig. 1a, which represents the shear span (i.e. ≈ half the length) of the member. Deformations of the cantilever are owing to flexure, shear action, and pullout slip of the reinforcement from the support. These response mechanisms are considered to act in series, therefore their effects are additive as reflected by the mechanical analogue used in calculations of deformation capacity (Fig. 1b): here the member itself develops elastic curvature over its length, contributing to the total drift, whereas all other effects (inelastic rotation over the plastic hinge region, shear deformation and pullout slip) are modelled through pertinent springs, each contributing to the tip displacement of the cantilever (and therefore to drift) separately. These mechanisms were originally assumed to act independently of each other, and therefore, the total deformation obtained for any given load combination was approximated by the summation of the individual contributions of the participating mechanisms; resistance curves were established for each mechanism from first principles (Fig. 2). The shear force sustained by each mechanism and the corresponding deformation or drift of the cantilever (drift is the chord rotation of the member with respect its original orientation), follow the relationship:

$$V=V_{fl}=M/L_s=V_{sh}=V_{sl};\quad D= D_{fl}+ D_{sh}+ D_{sl} \tag{1}$$

The same concept has been extended to *deformation capacity* (a measure of total deformation that the member may undergo without significant irreversible loss of strength; by international convention lateral drift or deformation capacity are values associated with a 20% loss of strength beyond the peak point.) The result of Eq. 1 has been tested against hundreds of tests contained in a number of databases, including R.C. members with modern detailing as well as members with substandard details representative of old design practices (Inel 2002, Panagiotakos 2001, Syntzirma 2002). The success of the approach is limited to estimations of realistic values for well detailed members, which generally demonstrate quite high deformation capacity particularly when their axial load ratio is less than 0.4. Values become irrelevant when this concept is applied to members experiencing premature modes of failure, such as often encountered with old-type frame members. Clearly, if the strength of one of the springs in the assembly of Fig. 1b is overcome at some value of deformation, then this event terminates the response curve of the member, well before the development of the estimated nominal deformation capacity of the other springs. For this reason, the approach underlined by Eq. 1 has been retained of late, only to describe behavior up to the onset of yielding, i.e. $q_y=q_y^{fl}+q_y^{sl}+q_y^{sh}$. For response beyond yielding, opinions diverge as to how to estimate deformation capacity. Thus, the revised ASCE-41 document (Elwood 2007) evaluates directly the total inelastic drift capacity, q_u, through empirical rules, the result being a single compound value that accounts for the various effects and design parameters through pertinent binary rules: here, the total rotation capacity is $q_u = q_y + q_{pl}$. Similar is the approach drafted for the next round of EC8-III (2005), which provides direct estimates for the total inelastic rotation capacity q_u through calibrated expressions in terms of the relevant design variables. A summary of the essential elements of both approaches for calculation of drift or rotation capacity is outlined in the Appendix of this paper.

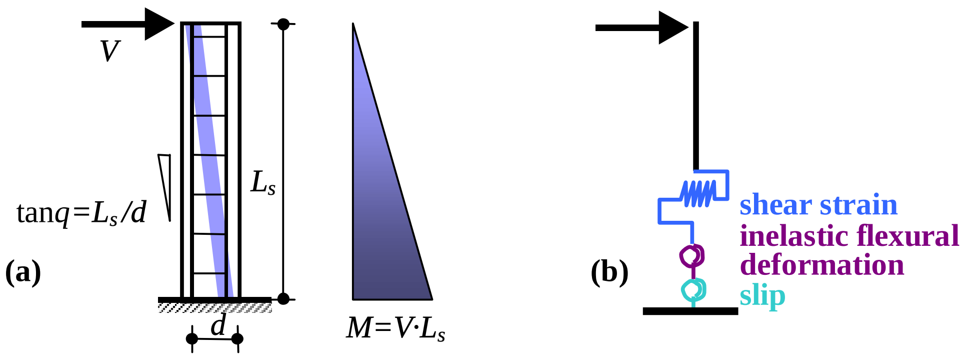

Figure 1. (a) Cantilever model and moment distribution, (b) Mechanisms of behaviour modelled through pertinent springs

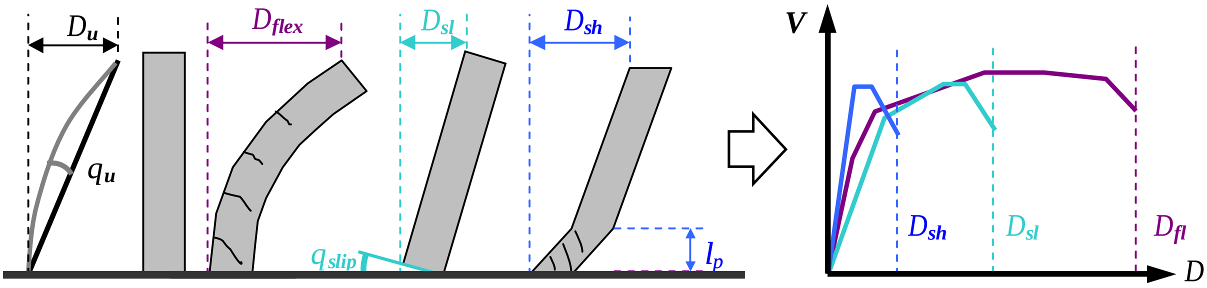

Figure 2. Contribution of the various response mechanisms to the total drift

Recognizing the fundamental relevance of the model depicted in Fig. 1b the authors attempted to improve on the correlation of Eq. 1 with the test data, by modifying the expression: contributions of the individual contributing mechanisms were scaled to the onset of occurrence of any type of premature failure (Syntzirma 2006). The framework was referred to as Capacity - Based Prioritizing (CBP) of failure modes. Cantilever strength values associated with failure of each individual response mechanism of resistance in the spring-series of Fig. 1, namely Flexural ($V_{u,fl}$), Shear ($V_{u,sh}$), Anchorage/Lap Splice ($V_{u,sl}$), or Compression Bar Stability ($V_{u,buckl}$) are considered in establishing the hierarchy of member failure, with the lower strength spring controlling the mode of damage and possibly, failure of the member. Thus, V_{fail} is defined by,

$$V_{fail} = \min\{V_{u,fl}, V_{u,sh}, V_{u,sl}, V_{u,buckl}\} \tag{2}$$

and it is then used to estimate the weight w_u in the amended expression for deformation capacity:

$$q_y = w_y \left[q_{y,fl} + q_{y,sh} + q_{y,sl} \right]; \; q_u = q_{y,fl} + w_u \left[q_{p,fl} + q_{p,sh} + q_{p,sl} \right] \tag{3}$$

Subscripts y and u correspond to yield and ultimate states; q and D are the drift and displacement of the element. Factors w_y, w_u represent strength ratios for strength-controlled mechanisms of behaviour or deformation ratios for strain-controlled mechanisms of behaviour. For example, if $V_{u,sh}=V_{fail}<(V_{u,fl}\,;\,V_{u,sl})$, then $w_y=V_{fail}/V_{u,fl}<1$ and $q_u=q_y$, whereas if $w_y=1$, then, $w_u=(m_{fail}-1)/(m_{fl}-1)$, where m_{fail} is the displacement ductility corresponding to the point when the reduced values of either of the nominal strengths of the shear and slip mechanisms, $V_{u,sh}$ or $V_{u,sl}$ become equal to the flexural strength $V_{u,fl}$ (Fig. 2), and m_{fl} is the theoretical available ductility of the member when considering full flexural action. (Here reference is being made to the value of nominal strength terms which are considered to decay with increasing imposed ductility, m. Even when flexural yielding is possible for m=1, the relative hierarchy of the strength terms may be reversed for larger m values, since they decay at different rates. In the above a simplification has been made, whereby all plastic displacement components have been assumed to increase proportionally with ductility; a summary of the essential components of this approach is outlined in the Appendix.)

Parametric study

A comparative study of the estimates obtained from the CBP procedure outlined above and from the two reference assessment standards (ASCE-41, EC8-III) is conducted on a series of column-elements representative of field assessment examples; most cases have reinforcing details according with former detailing practices (i.e. sparse stirrups, with inadequate anchorage or lap-splice of long. reinforcement etc.) The collection of cases considered is depicted in Fig. 3, and has been designed to systematically test the performance of analytical methods for deformation capacity estimation with respect to all those design variables that could prematurely cause member failure and should therefore be explicitly accounted for in the evaluation study. Thus, column (a) represents the basic case study having a 350mm×400 mm cross section; two cases of longitudinal reinforcement are considered, namely either 8, 18mm diameter bars (4 bars on each side of the cross section) or 4, 18 mm diameter bars (2 bars on each side of the cross section); transverse reinforcement comprises rectangular stirrups with 8mm diameter at a spacing of either 100 or 200 mm; stirrups are anchored either with 135^0 or with 90^0 hooks. Another variable is the normalized axial load v (=the applied axial load divided by the column cross section A_g and the concrete strength f_c'), taken here either equal to v=0.1 or equal to v=0.35. Reference material properties are, concrete strength f_c'=20MPa, S500 steel for longitudinal reinforcement (f_y=500MPa), whereas transverse reinforcement comprises S220 (f_y=220MPa).

Column (b) in Fig. 3 has been derived from (a) by introducing a short lap-splice (=15D_b) of longitudinal reinforcement at the base; case (c) derives from (a) but has a short length (=15D_b) of embedment of primary reinforcement; case (d) is identical to (a) but due to half-height masonry infills, it is expected to function as a captive column; (e) has a 700mm deep cross section (i.e. a lower aspect ratio than (a)); similarly, case (f) with a construction hinge at the base has twice the aspect ratio of (a). Since all possible combinations of detailing characteristics seen in case (a) are also considered in cases (b)-(f), a very large number of possible situations are evaluated with the three models considered; results are presented in Figs. 4-9, in the form of bar-charts. Each group of bars in the typical chart corresponds to the estimated rotation capacity for the respective column, obtained with the alternative models (blue for the CBP mechanical model, purple for the ASCE-41 Model, and beige for the EC8-III model), for each case study considered. For easy reference the following system of case identification is used in the remainder of this presentation: the first numeral in the I.D. code represents the aspect ratio, i.e., the shear span to the height of the cross section ratio, L_s/h. Next C, A, S or H for: adequately anchored continuous reinforcement (***C***), poorly anchored (***A***), or lap-spliced (***S***) longitudinal reinforcement at the base of the column above the footing, or a hinge-type (***H***) primary reinforcement arrangement. Letter ***L*** or ***M*** identifies cases with a light (*n*=0.1) or moderate (*n*=0.35) axial load ratio; this is followed by the number of longitudinal bars (integer 4 or 8). Last the code gives the spacing and anchorage detail of transverse stirrups. For example, the identification code 3.75CL8/200-135 refers to a type (a) column with a *light* axial load, a 400mm high cross section, *8* longitudinal bars (D_b=18 mm), rectangular stirrups spaced at *200mm* and anchored with *135^0* hooks.

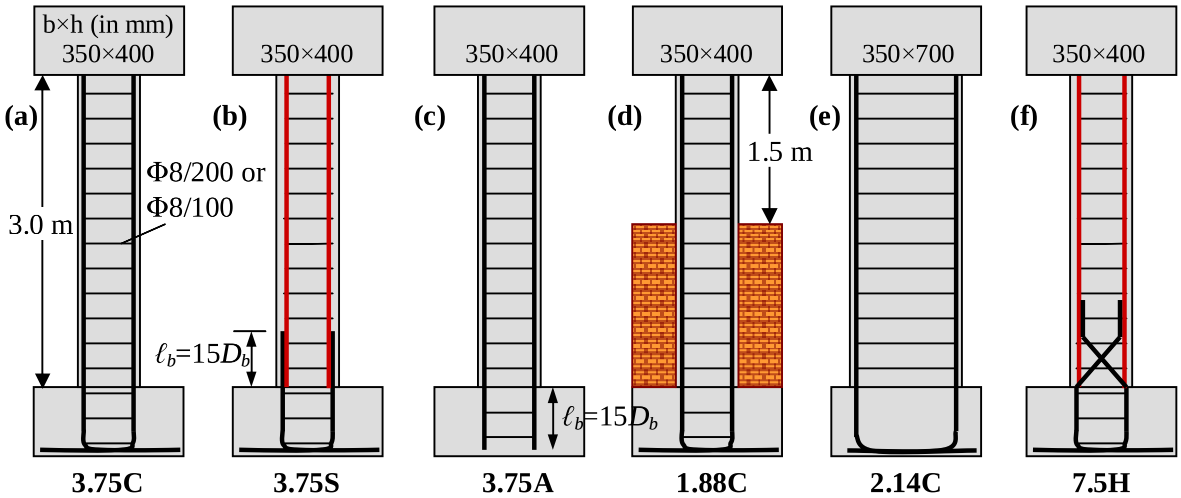

Figure 3. Benchmark problems used in the comparative parametric study

Each of the figures summarizing the results contains 16 bar groups in the horizontal axis: the first eight correspond to the low axial load ratio (*v*=0.1), whereas the other eight correspond to the moderate axial load ratio (*v*=0.35). In each of the eight cases within the two subgroups, cases are organized in the horizontal axis with the sequence shown in Fig. 4b. Comparative plots give the terms of Eq. (2) namely $V_{u,fl}$, $V_{u,sh}$, $V_{u,sl}$ and the deformation capacity indices q_y and q_{pl}.

Note that all models consistently estimate a significant reduction in the response terms associated with the moderate axial load ratio (second group of eight cases considered, as opposed to the first group). Owing to the "cutoff" region in the ASCE-41 and EC8-III which is used for flexural cases with low axial load ratio, the substantial deformation capacity of column 7.5H for the case of 4Φ18 longitudinal reinforcement and with spacing of stirrups 100mm with 90^0 hooks as calculated from the mechanistic approach presents an excessive value as compared to the code – recommended values. In many cases the approaches converge, particularly when the governing mode of failure is flexural. Deviations occur in cases where the prevailing mode is related to some form of anchorage or lap splice failure, either direct, or after sustained flexural yielding and subsequent yield penetration; deviations are also noticeable in expressions estimating the shear strength. These are the axes where further calibration and refinement of deformation capacity models is needed, to achieve improved estimates from the code expressions, consistent with the mechanistic models and the available experimental trends.

CONCLUSIONS

A Benchmark test is proposed for parametric evaluation of the sensitivities of mechanistic and code-based models used in calculating the deformation capacity of substandard reinforced concrete members (i.e., lightly reinforced members representative of older practices). It is worth noting that simplification of the process by elimination of criteria concerning some less understood modes of failure such as yield penetration after flexural yielding, debonding of the cover due to reversal of concrete cover strains etc. is not always on the side of safety, an occurrence that may be easily identified from systematic use of the Benchmark evaluation.

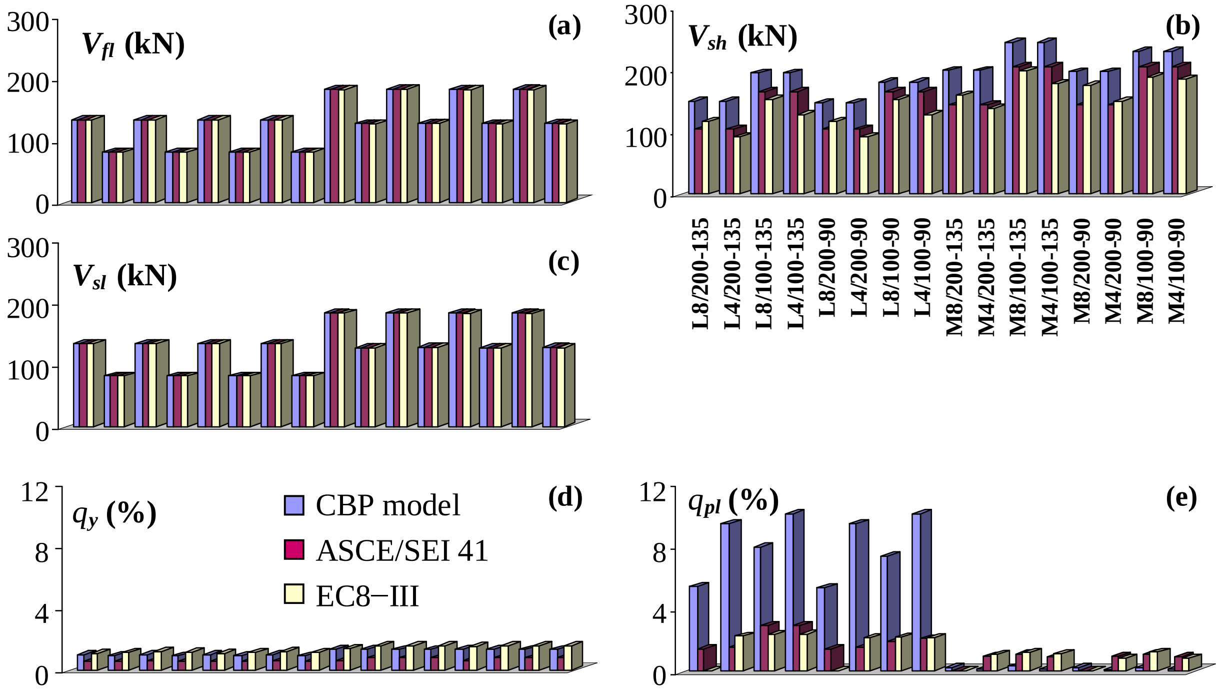

Figure 4. Parametric analysis for specimen 3.75C

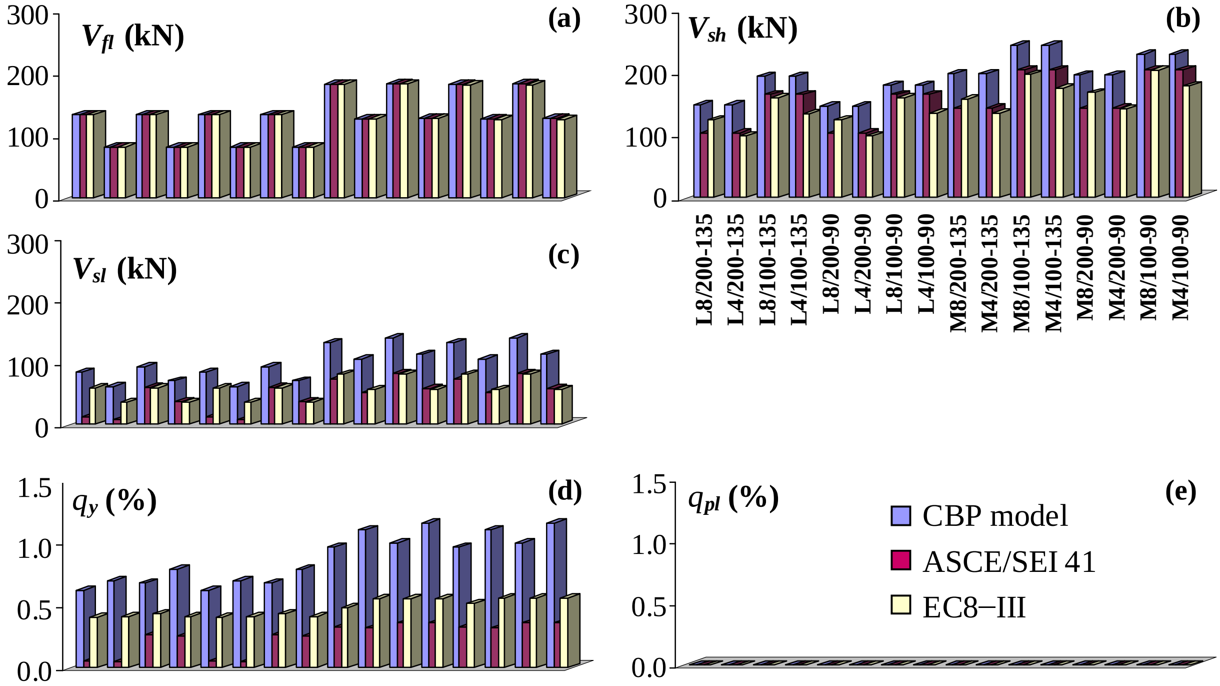

Figure 5. Parametric analysis for specimen 3.75S

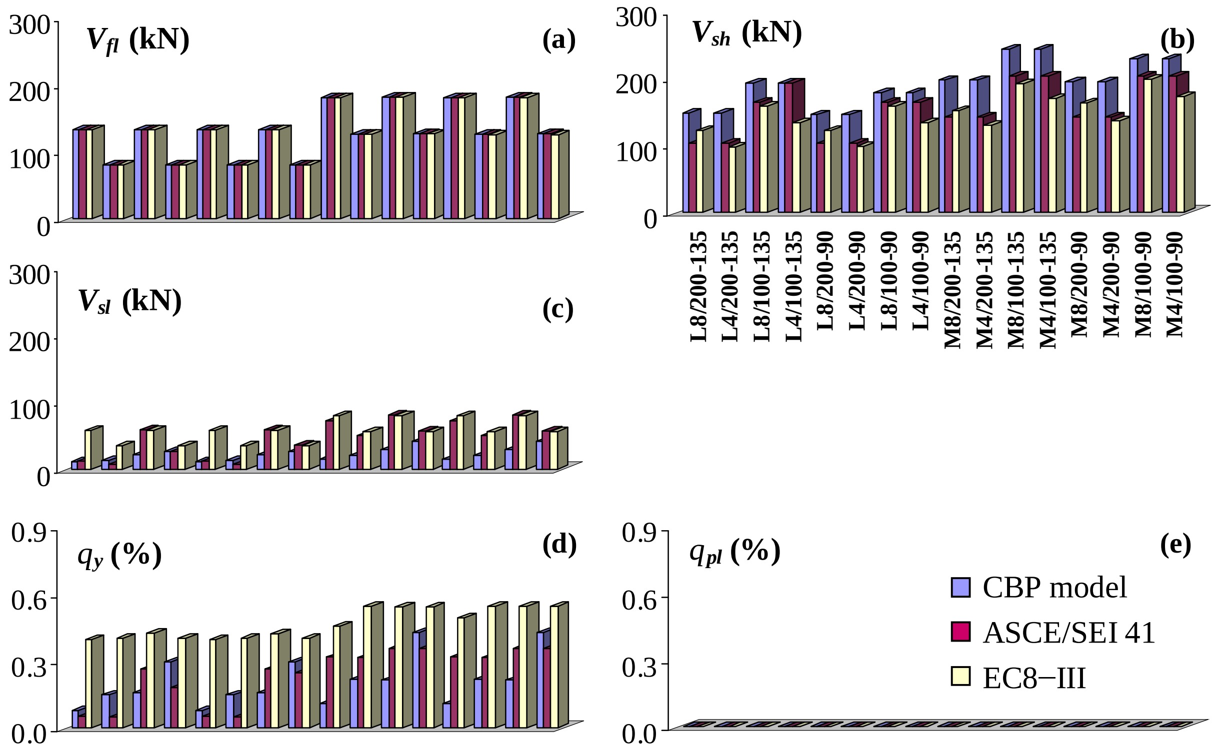

Figure 6. Parametric analysis for specimen 3.75A

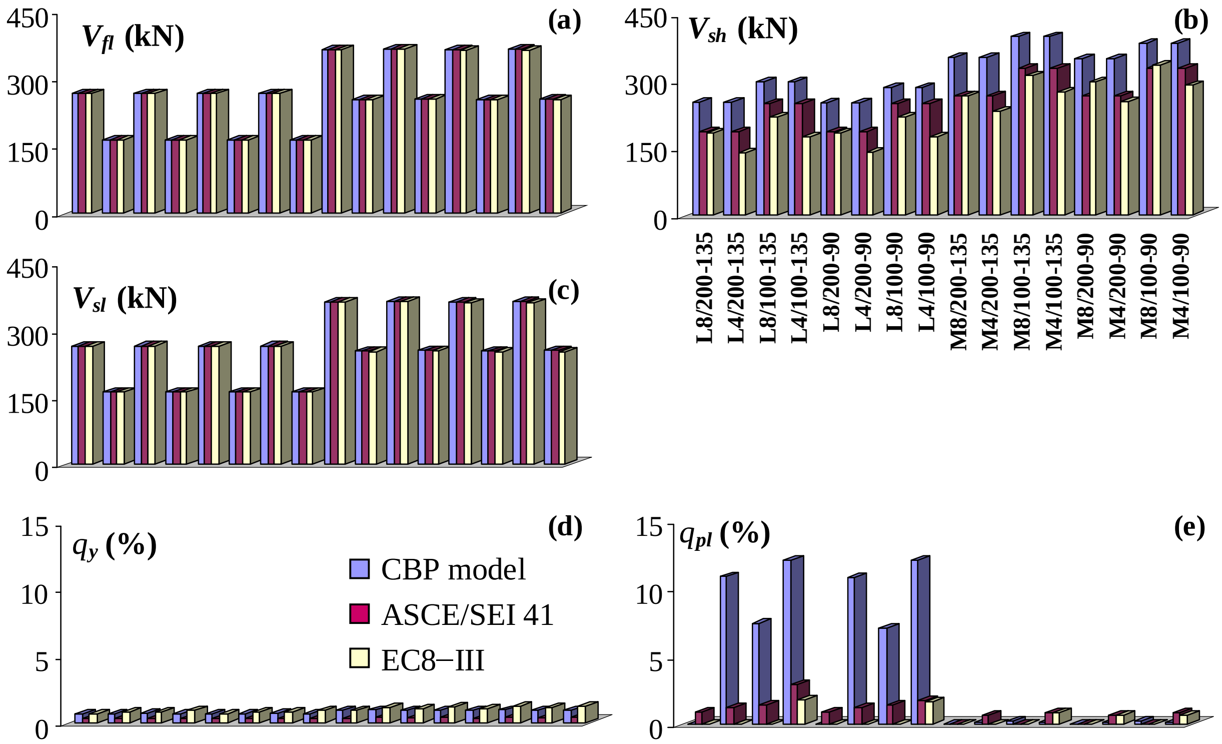

Figure 7. Parametric analysis for specimen 1.88C

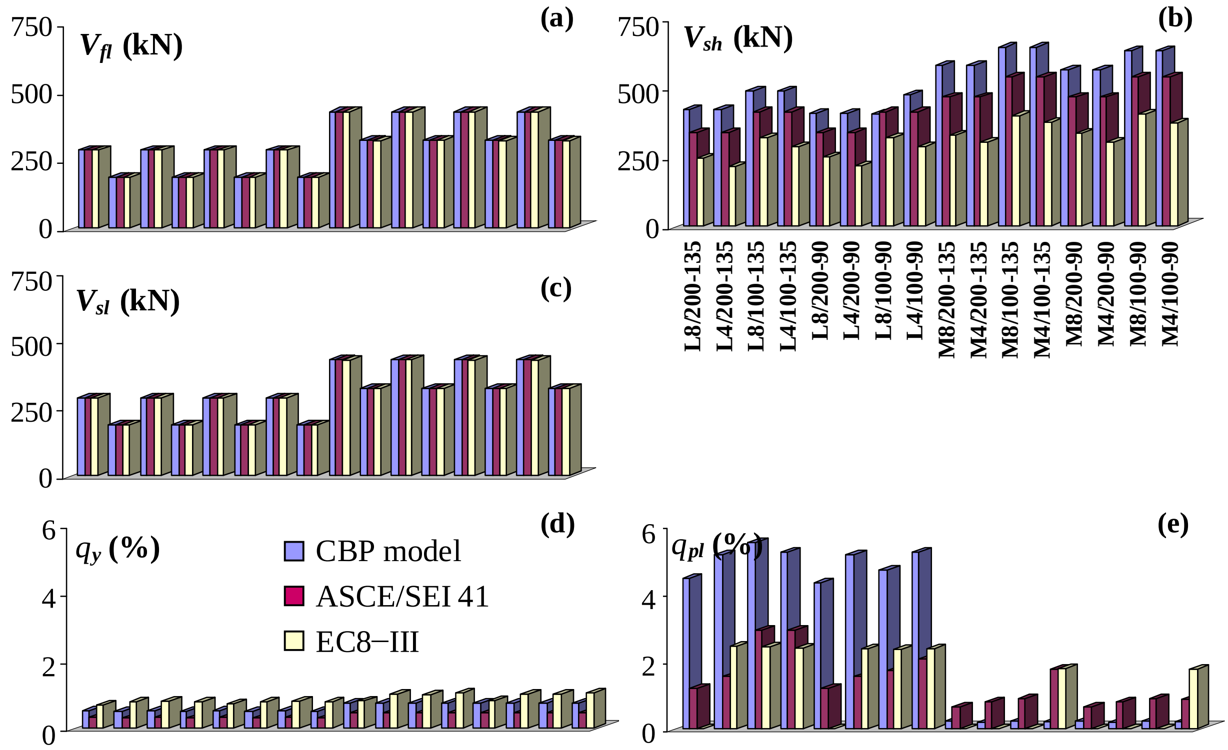

Figure 8. Parametric analysis for specimen 2.14C

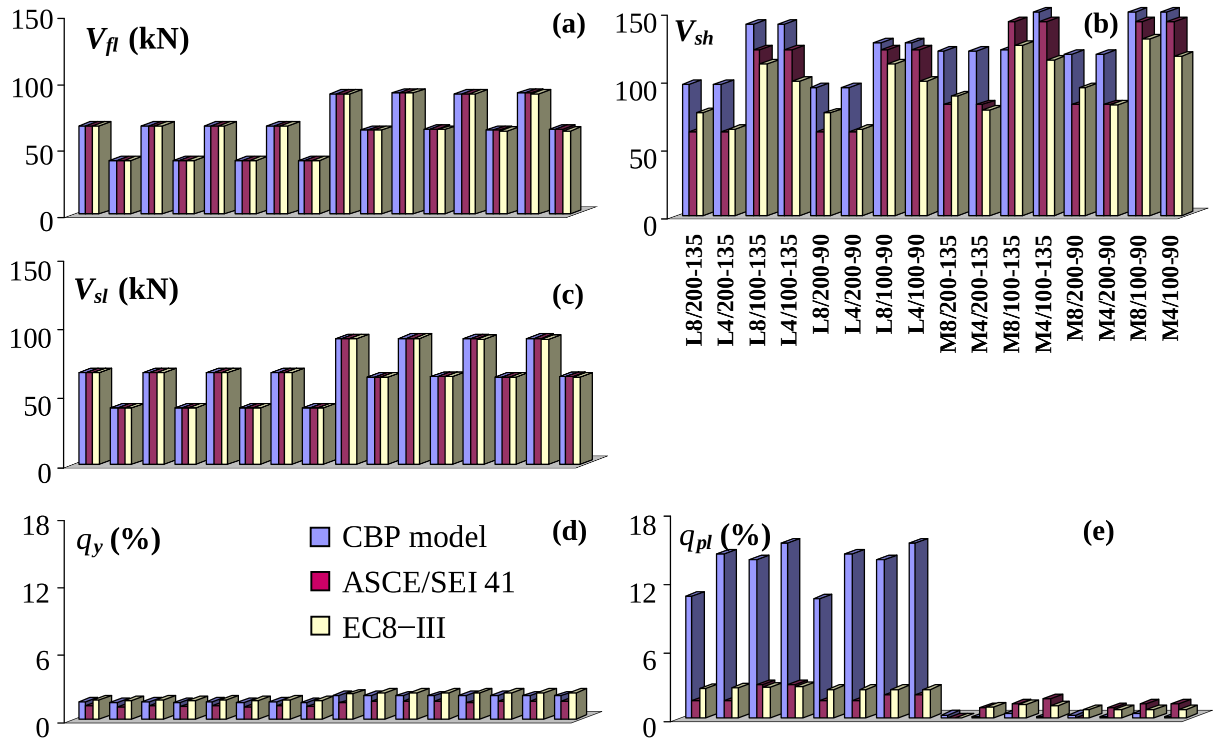

Figure 9. Parametric analysis for specimen 7.5H

Appendix

ASCE/SEI-41

For concrete: e_{co}=0.002 and e_{cu}=0.005; for steel e_{su}=0.05; f_u=1.25f_y

Conforming elements: $s \le d/3$ and $V_s \ge 0.75V_n$

Shear strength: $$V_c = k(m_\Delta)\left[\frac{0.5\sqrt{f_c}}{L_s/d}\sqrt{1+\frac{N}{0.5A_g\sqrt{f_c}}}\right]0.8A_g$$

$$V_s = k(m_\Delta)\left[\frac{A_{sw} f_{yh} d}{s}\right]; \quad \text{if } s \ge d/2 \Rightarrow 0.5V_s; \quad \text{if } s \ge d \Rightarrow V_s = 0$$

$$\text{for } m_\Delta \le 2 \to k = 1.0; \quad \text{for } 2 < m_\Delta \le 6 \to k = -0.1m_\Delta + 1.2; \; \text{for } m_\Delta > 6 \to k = 0.6$$

Longitudinal Reinf.: $$f_s = 1.25z\, f_y\left(\frac{L_{d,\,avail}}{L_d}\right)^{2/3}; \quad \frac{L_d}{D_b} = \frac{1.25f_y}{B\sqrt{f_c}}; \quad \begin{bmatrix} B=2 \text{ for } D_b \le N.6 \\ B=1.66 \text{ for } D_b \ge N.7 \\ B=5.4 \text{ for } 90^o \text{ hooks} \end{bmatrix}$$

$k(m_D)\chi V_{flex}/V_n$		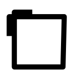
≤0.6 & $A_{sw}/b_w s$>0.2%; s/d<0.5	F.F.	F. F.– S. F.
≤1	F. F.– S. F.	S. F.
>1	S. F.	S. F.

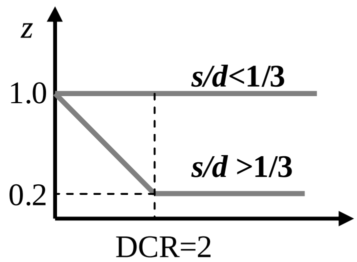

EC8-III

For concrete: e_{co}=0.002; e_{cu}=0.0035; e_{cu}^*=0.0035+$k_{eff} r_{sw} f_{yh}/f_c$’ but if 90^0 hoops ⇒ k_{eff}=0 and for steel e_{su}=0.075; f_u=1.15f_y

Shear strength: $$V_{shear} = k(m_\Delta)\cdot(0.16\cdot\max(0.5;100\,r_{tot})\cdot(1-0.16\min(5;\frac{L_s}{h})\cdot\sqrt{f_c}\cdot 0.8A_g)+$$

$$+\min\{N;0.55A_c f_c\}\cdot\tan a + k(m_\Delta)\cdot A_{sw}\cdot f_{yh}\cdot\left[\frac{d-d'}{s}\right]$$

for $m_D \le 5 \longrightarrow k = -0.05m_D+1.0$; for $m_D > 5 \longrightarrow k$=0.75

Drift components: $$q_y = \underbrace{\left(1/r\right)_y\frac{L_s + a_v z}{3}}_{q_{y,fl}} + \underbrace{0.00135\cdot\left(1+1.5\frac{h}{L_s}\right)}_{q_{y,sh}} + \underbrace{\frac{e_y}{z}\cdot\frac{D_b f_y}{6\sqrt{f_c}}}_{q_{y,sl}}$$

Variable a_v=0 if $V_{fl} < V_c$, otherwise a_v=1. If $V_{fl} > V_{shear}$ then q_y is reduced by multiplying by V_{sh}/V_{fl}.

$$q_{um}^{pl} = 0.014\cdot n_{1,pl}\cdot n_{2,pl}\cdot n_3\cdot n_4\cdot n_5 \quad \text{where } n_{1,pl} = 0.25^v; \; n_{2,pl} = f_c^{\,0.2}\cdot\left[\frac{\max(0.01, w')}{\max(0.01, w)}\right]^{0.3}$$

$$q_{um} = 0.016 \cdot n_{1,t} \cdot n_{2,t} \cdot n_3 \cdot n_4 \cdot n_5 \text{ where } n_{1,t} = 0.3^{\nu};\ n_{2,t} = \left[\frac{\max(0.01, w')}{\max(0.01, w)} \cdot f_c\right]^{0.225};\ n_3 = \left(\frac{L_s}{h}\right)^{0.35};$$

$$n_4 = 25^{a \cdot r_{sw} \cdot f_{yh} / f_c};\ n_5 = 1.25^{100 r_d}$$

Additional coefficients: for cold-formed steel n_6=0.5; for smooth bars: $n_{b,t}$=0.575, $n_{b,pl}$=0.375; for structures with brittle details: n_{old}=0.825, n_4=1; for lapped regions: double value of w' in n_2; whereas in case of deficient splices (ribbed bars): $n_L=L_{d,avail}/L_{d,min}$ where:

$$\frac{L_{d,\min}}{D_b} = \frac{f_y}{B\sqrt{f_c}} \text{ and } B = 1.05 + 14.5 \cdot k_{eff,L} \cdot r_{sw} \frac{f_{yh}}{f_c}$$

For lapped reinforcement the strain e_y and the stress f_y are obtained by multiplying with $L_{d,avail}/L_{d,min}$:

$$f_s = f_y \left(\frac{L_{d,avail}}{L_{d,\min}}\right);\quad L_{d,\min} = \frac{f_y \cdot D_b}{3.3\sqrt{f_c}}$$

C.B.P. model

For concrete: e_{co}=0.002 and e_{cu}=0.005; for steel e_{su}=0.05; f_u=1.25f_y; $e_{u,max}=e_y L_{anch}/L_{b,min}$

Shear strength: $$\text{if } \frac{N}{A_g \cdot f_c'} \geq (r_{s1} - r_{s2}) \frac{f_y}{f_c'} \rightarrow V_c = k(m_\Delta) \cdot 0.5\sqrt{f_c'} \cdot \left(\frac{d}{L_s}\sqrt{1 + \frac{N}{0.5\sqrt{f_c'} \cdot A_g}}\right) \cdot A_g;\ \text{otherwise } V_c = 0$$

$$V_s = k(m_\Delta) A_{st} \sum_{n_{st}} f_{st,i};\ n_{st} = d / s \text{ (int. part) but if hoops } 90^0 \rightarrow f_{st,i} = f_{y,st} L_{b,i} / 0.7 L_b$$

$$\text{for } m_\Delta \leq 2 \rightarrow k = 1.0;\ \text{for } 2 < m_\Delta \leq 6 \rightarrow k = -0.1 m_\Delta + 1.2;\ \text{for } m_\Delta > 6 \rightarrow k = 0.6$$

Lap-splice strength: $f_s = f_{steel} + f_{conc}$; $f_{steel}=1.4 A_{st} \cdot f_{yh} \cdot L_b/(s \cdot n_b \cdot A_b) \leq f_u$; $f_{conc}=(2.5 D_b + 2 d_{st} + 2c) \cdot f_t \cdot L_b / A_b$

References

Elwood K., Matamoros A., Wallace J., Lehman D., Heintz J., Mitchell A., Moore M., Valley M., Lowes L., Comartin C., Moehle J., (2007). "Update to ASCE/SEI 41 Concrete Provisions", *Earthquake Spectra*, 23(3), 493-523

FEMA 356, (2000). "Prestandard and commentary for the Seismic rehabilitation of buildings"

Eurocode 8, (2005). "Design of structures for earthquake resistance − Part 3: Assessment and retrofitting of buildings", *European Committee for Standardisation*

Inel M. and Aschheim M., (2002). "Displacement–Based Strategies for the Performance–Based Seismic Design of 'Short' Bridges Considering Embankment Flexibility", *CD release,* MAE Center, Univ. Illinois at Urbana-Champaign

Panagiotakos T., and Fardis M. N., (2001). "Deformation of R.C. Members at Yielding and Ultimate", *ACI Structural Journal*, 98(2), 135-148

Syntzirma D. V. and Pantazopoulou S. J., (2002), "Performance–Based Seismic Evaluation of R.C. Building Members", *CD-ROM Proceedings*, Paper Reference 816, 12th European Conf. on Earthq. Engineering, 9–13 Sept., London U.K.

Syntzirma D. V., Pantazopoulou S. J. (2006), "Deformation Capacity of R.C. Members with Brittle Details under Cyclic Loads", *ACI Special Publication* 236, 1-22